Kinetics and Mechanism of the Reaction of Cysteine and Hydrogen Peroxide in Aqueous Solution

DAYONG LUO,[1] SCOTT W. SMITH,[2] BRADLEY D. ANDERSON[1]

[1]Department of Pharmaceutical Sciences, University of Kentucky, Lexington, Kentucky 40506

[2]Pfizer Global Research and Development, San Diego, California 92121

Received 10 August 2004; revised 22 September 2004; accepted 22 September 2004

Published online in Wiley InterScience (www.interscience.wiley.com). DOI 10.1002/jps.20253

ABSTRACT: The oxidation of thiol-containing small molecules, peptides, and proteins in the presence of peroxides is of increasing biological and pharmaceutical interest. Although such reactions have been widely studied there does not appear to be a consensus in the literature as to the reaction products formed under various conditions, the reaction stoichiometry, and the reaction mechanisms that may be involved. This study examines the reaction kinetics of cysteine (CSH) with hydrogen peroxide (H_2O_2) in aqueous buffers (in the absence of metal ions) over a wide range of pH (pH 4–13) and at varying ratios of initial reactant concentrations to explore the range of conditions in which a two-step nucleophilic model describes the kinetics. The disappearance of CSH and H_2O_2 and appearance of cystine (CSSC) versus time were monitored by reverse-phase high-performance liquid chromatography (HPLC). The effects of oxygen, metal ions (Cu^{2+}), pH (4–13), ionic strength, buffer concentration, and temperature were evaluated. Data obtained at $[H_2O_2]_0/[CSH]_0$ ratios from 0.01–2.3 demonstrate that the reaction of CSH with H_2O_2 in the absence of metal ions is quantitatively consistent with a two-step nucleophilic reaction mechanism involving rate-determining nucleophilic attack of thiolate anion on the unionized H_2O_2 to generate cysteine sulfenic acid (CSOH) as an intermediate. Second-order rate constants for both reaction steps were generated through model fitting. At $[H_2O_2]_0/[CSH]_0 > 10$, the % CSSC formed as a product of the reaction declines due to the increased importance of alternative competing pathways for consumption of CSOH. A thorough understanding of the mechanism in aqueous solution will provide valuable background information for current studies aimed at elucidating the influence of such factors on thiol oxidation in solid-state formulations.

 J Pharm Sci 94:304–316, 2005

Keywords: cysteine; hydrogen peroxide; thiol oxidation; peptide stability; protein stability; nucleophilic substitution; disulfide formation; sulfenic acid; sulfinic acid; sulfonic acid

INTRODUCTION

The oxidation of peptide and protein pharmaceutical products has become an increasingly important problem in drug development as more biotechnology derived products progress toward clinical studies and commercialization.[1–3] Proteins containing one or more free cysteine residues (e.g., human serum albumin,[4] recombinant human α1-antitrypsin,[5] the superfamily of protein tyrosine phosphatases,[6,7] and a variety of others[8]), as well as thiol-containing peptides (e.g., glutathione[9,10] the angiotensin-converting enzyme inhibitor captopril[11] and the prostate-specific antigen peptides[12]) are particularly susceptible to thiol-oxidation through a variety of mechanisms. *In vitro*, these mechanisms may involve free-radical scavenging of various reactive oxygen species such as superoxide[9,10] or hydroxyl

Correspondence to: Bradley D. Anderson (Telephone: 859-257-2300, ext. 235; Fax: 859-257-2489; E-mail: bande2@email.uky.edu)

Journal of Pharmaceutical Sciences, Vol. 94, 304–316 (2005)

radical,[13] resulting in thiol loss and the consumption of oxygen. Alternatively, direct reaction of thiols via nucleophilic substitution with certain reactive oxygen species such as hydrogen peroxide may occur.[4,5,7,14,15]

Because of their reactivity as scavengers of reactive oxygen species, thiol-containing compounds can be highly effective as antioxidants for stabilizing pharmaceuticals.[13,16–20] However, this propensity toward oxidation makes formulation of proteins and peptides containing free cysteine residues more difficult. In pharmaceutical formulations, thiol autoxidation is generally thought to involve a series of complex reaction processes catalyzed by traces of transitional metal ions (e.g., Cu^{II} and Fe^{III}).[11,21–23] For this reason, metal ion chelators such as EDTA have proven to be effective stabilizers of thiol containing peptides and proteins.[24–26] Considering, however, that peroxides are also found as impurities in some common formulation excipients (e.g., polyvinylpyrrolidone, polyethylene glycol, polysorbate 80, etc.),[27–34] and that H_2O_2 is produced as a byproduct of metal-catalyzed oxidations,[35–37] an understanding of the mechanism of the thiol–H_2O_2 reaction is a prerequisite for understanding the general case of thiol oxidation in formulations.

Our interest in stabilizing thiol-containing peptides stems from recent attempts to prepare lyophilized prototype formulations of several prostate-specific antigen (PSA) peptides under consideration by the National Cancer Institute for vaccine therapy for human prostate cancer,[12,38] including the cys ras peptide (KLVVVGACGVGKS),[25] PSA-3 (VISNDVCAQV),[23,25] and PSA-OP (FLTPKKLQCVDLHVISNDVCAQVHPQKVTK).[26] Although EDTA was found to be highly effective in preventing metal-catalyzed disulfide formation in these lyophiles, the potential for the reaction of cysteine residues with trace peroxide impurities in excipients remains even in the presence of EDTA.

Several studies of the reaction between various low molecular weight thiols (e.g., cysteine, N-acetylcysteine, glutathione, and others) and hydrogen peroxide (H_2O_2) or other peroxides (e.g., benzoyl peroxide, lipid hydroperoxides, etc.) have been reported, but there does not appear to be a consensus as to the reaction products formed under various conditions,[10,14,15,39–42] the mechanism(s) by which these products form,[10,14,15,41–44] or the rate constants for various reaction steps.

This study examines the reaction kinetics of cysteine with H_2O_2 in aqueous buffers (in the absence of metal ions) over a wide range of pH (pH 4–13) and at varying ratios of initial reactant concentrations to explore the range of conditions over which a two-step nucleophilic model as depicted in Scheme I accounts for the reaction kinetics and stoichiometry. In aqueous solution the first step in Scheme I is rate-determining, but it may be possible to estimate rate constants for each process, depending on the extent to which the two reaction steps differ.

$$\mathrm{CSH} \underset{}{\overset{K_a}{\rightleftharpoons}} \mathrm{CS^-} + \mathrm{H^+}$$

$$1)\quad \mathrm{CS^-} + \mathrm{H_2O_2} \xrightarrow{k_1} \mathrm{CSOH} + \mathrm{HO^-}$$

$$2)\quad \mathrm{CSOH} + \mathrm{CS^-} \xrightarrow{k_2} \mathrm{CSSC} + \mathrm{HO^-}$$

Scheme I.

A thorough understanding of the mechanism of reaction between low molecular weight thiols and H_2O_2 in aqueous solution should be useful in rationalizing the fate of thiol-containing proteins undergoing reaction with hydrogen peroxide, where the buildup of the sulfenic acid intermediate (RSOH) suggests that the second reaction step may become rate-limiting in some circumstances. This may reflect the increased importance of reactant mobility in the second reaction step. Similarly, the reaction of the RSOH intermediate with a thiol residue in a second molecule of a thiol-containing peptide or protein may also become rate limiting in amorphous (e.g., lyophilized) pharmaceutical formulations that contain peroxide impurities. Evidence that the disulfide may not be the sole reaction product under certain conditions led to an exploration of the possible factors influencing the fate of the sulfenic acid intermediate (RSOH) and the reaction products ultimately formed when RSOH reacts with H_2O_2 or another molecule of RSOH.

EXPERIMENTAL

Reagents

Cysteine (>98% purity by TLC), cystine (Sigma-Ultra, >99% purity by TLC), cysteine sulfinic acid (water content 1 mol/mol), cysteic acid (monohydrate), and ethylenediaminetetraacetic acid (EDTA) were purchased from Sigma Chemical

Co. (St. Louis, MO). H_2O_2 (30% aqueous solution) and cupric sulfate ($CuSO_4 \cdot 5H_2O$) were obtained from Mallinckrodt Baker Inc. (Phillipsburg, NJ). All reagents were analytical grade and used as supplied. Deionized ultra-filtered (DIUF®) water used to prepare CSH and H_2O_2 solutions and HPLC grade acetonitrile were purchased from Fisher Scientific Co. (Pittsburgh, PA). Water used in mobile phase was deionized and further purified through a Milli-Q® UV Plus Ultrapure Water System, Millipore Ltd. (Billerica, MA).

High-Performance Liquid Chromatography (HPLC)

The analyses of CSH, CSSC, and H_2O_2 were carried out by reverse-phase high-performance liquid chromatography (HPLC). The system consisted of a Beckman 110A Solvent Delivery Module (Beckman Coulter, Fullerton, CA), a Waters™ 717 plus Autosampler (Waters Corp., Milford, MA), and a Hewlett-Packard 1040M Series II HPLC detector (Hewlett-Packard Company, Palo Alto, CA) operating at 214 nm, which was connected to a PC for data acquisition and analysis using HP LC/MSD ChemStation software. A Supelcosil ABZ+Plus, 5-μm (250 × 4.6 mm) (Supelco, Bellefonte, PA) analytical column and 5 μm (2 cm × 2.1 mm) guard column were employed. Elutions were performed isocratically using a mobile phase consisting of 50% (v/v) of an aqueous solution of 50 mM phosphoric acid (solution A) and 50% (v/v) of a solution containing 5 mM sodium 1-nonanesulphonate (99%, Lancaster Synthesis, Inc., Windham, NH), 50 mM phosphoric acid, and 5% (v/v) acetonitrile in water (solution B) at a flow rate 1.5 mL/min. Solution B was also used as the quench solution. The pH of the mobile phase was adjusted to 2.5 with NaOH. The retention times for H_2O_2, CSH, and CSSC were ~2 min, ~4.8 min, and ~6.5 min, respectively. Cysteine sulfinic acid (CSO_2H) and cysteic acid (CSO_3H) eluted prior to H_2O_2 at ~1.8 min, but could not be adequately resolved for quantitation purposes under these conditions. Separations of CSO_2H from CSO_3H required two Supelcosil ABZ+Plus columns connected in series and a flow rate of 0.5 mL/min. Under these conditions, retention times for CSO_2H and CSO_3H were ~10.4 and ~11 min, respectively.

General Procedure for Kinetic Studies

Fresh stock solutions of CSH were prepared by weighing ~20 mg CSH into a 1.5-mL plastic microcentrifuge tube (VWR Scientific Products Co., Buffalo Grove, IL) and dissolving in 1 mL phosphate buffer prepared from phosphoric acid solution (50 mM) adjusted to the desired pH with sodium hydroxide. Stock solutions of H_2O_2 were prepared by combining 0.1 mL 30% aqueous H_2O_2 solution and 0.9 mL of the same phosphate buffer (50 mM) in a 1.5-mL plastic microcentrifuge tube.

Reactions were initiated after first diluting the above stock solutions with the same buffer to a concentration twice that in the final reaction, equilibrating to the desired reaction temperature in a water bath set at 25°C. Equal volumes of each diluted solution were then combined by adding the diluted H_2O_2 solution to the CSH solution and rapidly mixing in a 15 mL plastic centrifuge tube (Falcon®, Becton Dickinson Co., Franklin Lakes, NJ). Reaction solutions were stored at 25°C and aliquots (0.1 mL) were taken at predetermined time intervals and transferred into 1-mL HPLC vials. An aliquot of 0.1-mL solution B was added to quench the reaction by lowering the pH and the total volume was adjusted to 1 mL with the mobile phase. Samples were analyzed immediately by HPLC.

Kinetic studies to obtain a preliminary assessment of reaction order, metal ion effects, and the influence of oxygen utilized the initial rate method whereby the formation of cystine was monitored at several time points in the very early stages of the reaction (first minute) at varying initial concentrations of CSH and H_2O_2. More comprehensive studies for use in fitting mathematical models to the data (see Data Analyses), generating pH-rate profiles, and examining the effects of buffer concentration and ionic strength involved the determination of complete reactant (i.e., CSH and H_2O_2) and product concentration versus time profiles.

Metal Ion and Oxygen Effects

Solutions containing equal (5 mM) concentrations of CSH and H_2O_2 and varying in EDTA concentration (0, 25, and 50 mM) were prepared by combining stock solutions in pH 6.0 (50 mM) sodium phosphate buffer either with or without addition of 50 μM cupric sulfate ($CuSO_4$). Buffers employed in the absence of added cupric ion were prepared using either Milli-Q treated deionized water or DIUF® water (see Reagents).

The influence of oxygen was explored using initial rate studies both in air-equilibrated samples and samples prepared and stored under a nitrogen atmosphere (in a glove box). Sample

temperatures were controlled by placing samples in a water jacketed container at 25°C. An OM-4 oxygen meter (Microelectrodes, Inc., Bedford, NH) was used to verify the removal of oxygen from diluted stock solutions that were bubbled with nitrogen prior to being combined to start a given reaction. The oxygen meter was calibrated by adjusting the reading to 0% in buffer solutions treated by bubbling with a N_2 stream for more than 30 min (only 20 min was necessary to achieve a constant reading) and to 100% in oxygen saturated buffer solutions. Experiments were at pH 6.0 and at a fixed starting concentration of CSH (25 mM) while H_2O_2 starting concentrations were varied (i.e., 5, 10, 25, and 50 mM) or a fixed starting concentration of H_2O_2 (10 mM) while CSH starting concentrations were varied (i.e., 2, 5, 10, and 25 mM).

Buffer, Ionic Strength, pH, and Temperature Effects

Phosphate buffers (pH 7) were prepared at different buffer concentrations (10, 30, and 50 mM) and at a constant ionic strength of 0.5 M (adjusted with sodium chloride (NaCl)). The kinetics of reaction in solutions containing 4 mM CSH and 4 mM H_2O_2 were monitored as a function of buffer concentration and second-order reaction rate constants generated through model fitting were compared.

The effect of ionic strength was explored by comparing the kinetics of reaction between 4 mM CSH and 4 mM H_2O_2 in 50 mM sodium phosphate buffers at pH 5.0, 7.0, 10.0, and 13.0 either in the absence of added NaCl or in buffers adjusted to an ionic strength of 0.5 M with NaCl. Second-order rate constants generated through model fitting of the experimental data were then compared.

The influence of pH on the reaction between 4 mM CSH and 4 mM H_2O_2 was monitored in buffers ranging from pH 4–13 at 25°C. Buffers were prepared with 50 mM phosphoric acid solution and sodium hydroxide (NaOH). Ionic strength was not adjusted. The observed reaction rate constants (k_{obs}) obtained through the model fitting of the experimental data were employed to construct the pH-rate profile.

Reactions between CSH and H_2O_2 were conducted at different temperatures (0, 25, and 50°C) in pH 6.0 buffer solution using an ice bath for 0°C, a water bath at 25°C and an oven at 50°C. Rate constants (k_1) generated from model fitting (see Data Analysis) were then fit to the Arrhenius equation to obtain an estimate for the energy of activation.

Effect of $[CSH]_0/[H_2O_2]_0$ Ratio on Kinetics and Reaction Products

To further explore the range of applicability of the simple nucleophilic mechanism depicted in Scheme I, additional experiments were carried out in which the ratio of starting concentrations of CSH and H_2O_2 ($[CSH]_0/[H_2O_2]_0$) was varied from 100 to 0.001. A ratio of $[CSH]_0:[H_2O_2]_0 = 100$ using 50 mM CSH and 500 μM H_2O_2 at pH 6.0 was employed to assess the effect of a large excess of CSH on the rate of disappearance of H_2O_2. The effects of $[CSH]_0:[H_2O_2]_0$ ratios $\ll 1.0$ (i.e., 1 to 0.001) were evaluated at pH 5.0, 6.0, and 7.0 to explore the possible generation of new reaction products in the presence of excess H_2O_2. The concentration of $[CSH]_0$ in these experiments was 3 mM at $[CSH]_0:[H_2O_2]_0$ ratios of 1 and 0.5 and 1 mM at ratios between 0.2 and 0.001. Solution aliquots were taken after the reactions were complete (72 h at pH 7.0, 96 h at pH 6.0, and 120 h at pH 5.0) and analyzed by HPLC for the CSSC product formed during the reaction. Analyses of some of the samples at later time points verified that the CSSC concentrations did not change after completion of the reaction.

DATA ANALYSIS

Concentration versus time curves for the disappearance of CSH and H_2O_2 and appearance of CSSC were fit to a mathematical model derived from Scheme I using nonlinear least-squares regression analysis (SCIENTIST®, Micromath Inc., Salt Lake City, UT) to obtain estimates for the two second-order rate constants, k_1 and k_2. The following differential equations can be generated from Scheme I:

$$\frac{-d[CS^-]}{dt} = k_1[CS^-][H_2O_2] + k_2[CS^-][CSOH] \quad (1)$$

$$\frac{-d[HOOH]}{dt} = k_1[CS^-][H_2O_2] \quad (2)$$

$$\frac{d[CSOH]}{dt} = k_1[CS^-][H_2O_2] - k_2[CS^-][CSOH] \quad (3)$$

$$\frac{d[CSSC]}{dt} = k_2[CS^-][CSOH] \quad (4)$$

where [CS^-], [H_2O_2], [CSOH], and [CSSC] are the concentrations of cysteine thiolate anion, hydrogen peroxide, the cysteine sulfenic acid intermediate, and cystine, respectively, at time t.

RESULTS AND DISCUSSION

Simultaneous analysis of CSH, H_2O_2, and CSSC by HPLC

The reaction between CSH and H_2O_2 has been previously studied by several other groups.[10,14,43,45] Normally in these studies, the concentrations of thiol and H_2O_2 were measured by colorimetric methods and CSSC concentration was not analyzed. Although HPLC methods to separate CSH and CSSC[46] and to separately determine H_2O_2 concentration in various media[34,47] have been reported, we are not aware of attempts to analyze all three reaction components in a single HPLC method. Figure 1 displays typical HPLC chromatograms obtained during the reaction of CSH with H_2O_2 leading to the formation of CSSC. Response factors were verified to be linear for all three compounds over concentration ranges of 0.025–2.5 mM for CSH, 0.1–10 mM for H_2O_2, and 3–400 μM for CSSC (solubility limited the range for CSSC) with intraday precision of <1% for all analytes. Interday precision in response factors was 1.6, 1.3, and 6.6% for CSH, H_2O_2, and CSSC, respectively. Detection limits at 214 nm estimated from three times the standard deviation for the lowest concentrations analyzed were 1.4 μM (0.14 nmol), 6.5 μM (.65 nmol), and 0.3 μM (0.03 nmol), respectively, for CSH, H_2O_2, and CSSC. These detection limits indicate that HPLC detection at 214 nm is not as sensitive for H_2O_2 as methods using electrochemical detection[34] nor as sensitive for CSH and CSSC as HPLC with coulometric detection.[46] However, Vignaud et al.[46] have observed that UV detection is more stable and easier to handle.

Elimination of Metal Ions and Oxygen as Variables in the Kinetic Studies

Because autoxidation of CSH (i.e., the direct reaction between CSH and molecular oxygen) is a spin-forbidden process, this reaction was not expected to contribute to the kinetics in this study.[48] However, the presence of trace of transition metal ions will significantly accelerate thiol autoxidation. Transition metal ions such as Cu^{2+} and Fe^{3+} not only catalyze autoxidation, but also act as direct oxidants in thiol oxidation.[22,36,37,49–52] Given the above, it is clear that transition metal ions had to be avoided to minimize the contribution of alternate routes of thiol oxidation.

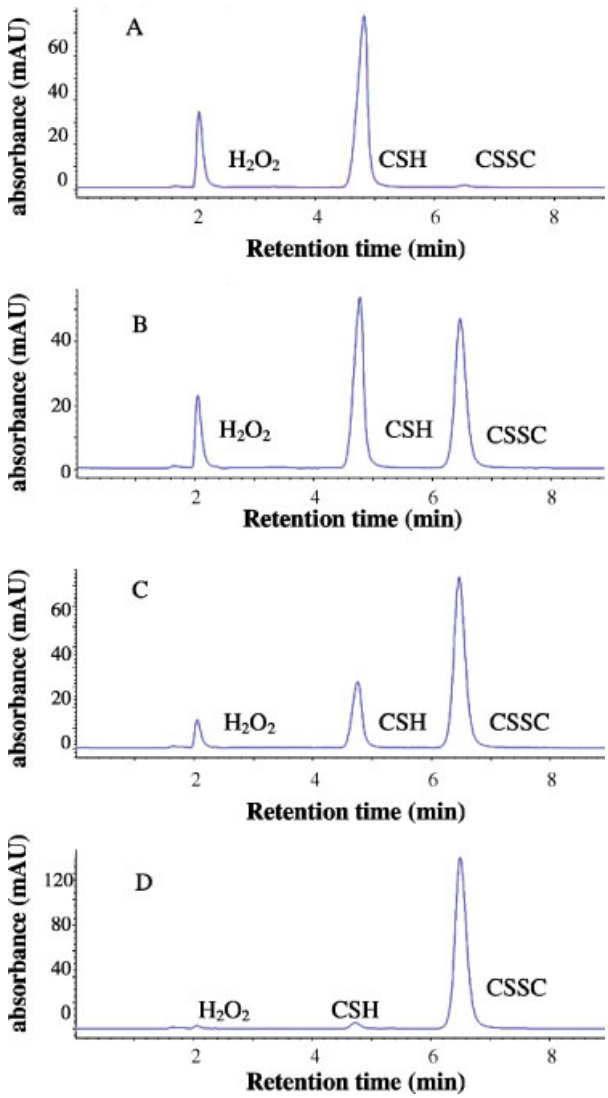

Figure 1. HPLC chromatograms (214 nm) at various times during the reaction of CSH with H_2O_2. Conditions: $[CSH]_0 = 4$ mM, $[H_2O_2]_0 = 2$ mM in pH 6.0 (50 mM) phosphate buffer at 25°C. Times: (A) 15 s; (B) 30 min; (C) 90 min; (D) 900 min. [Color figure can be seen in the online version of this article, available on the website, www.interscience.wiley.com.]

The ability of the metal ion chelator EDTA to eliminate the effect of metal ions on the reaction between CSH and H_2O_2 was investigated in pH 6.0 solutions containing equal (5 mM) concentrations of CSH and H_2O_2 and varying in EDTA concentration (0, 25, and 50 mM) either with or without the addition of 50 μM cupric sulfate ($CuSO_4$). Initial rates of formation of CSSC, shown in Figure 2,

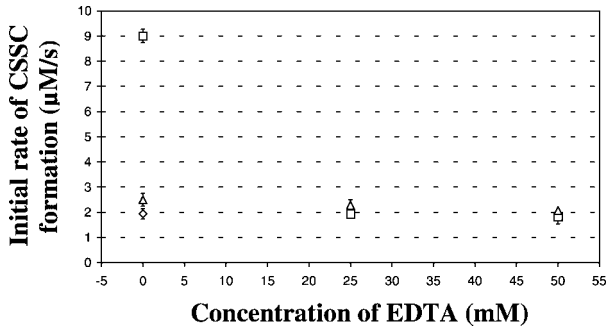

Figure 2. Initial rates of CSSC formation in solutions containing equal (5 mM) concentrations of CSH and H_2O_2 versus EDTA concentration (0, 25, and 50 mM) in pH 6.0 (50 mM) sodium phosphate buffer either with (□) or without (△, ◇) addition of 50 μM cupric sulfate ($CuSO_4$). Buffers employed in the absence of added cupric ion were prepared using either Milli-Q treated deionized water (△) or commercially obtained deionized ultrafiltered (DIUF®) water (◇).

indicate that the addition of cupric ion (Cu^{2+}) dramatically increases the reaction rate in the absence of EDTA, but that addition of EDTA suppresses this effect. In the presence of 25 mM EDTA, the rate of CSSC formation with the addition of Cu^{2+} is identical to the rate in deionized water containing no added cupric ion. EDTA addition had no apparent effect itself on the reaction rate in the absence of added metal ion but did interfere with the HPLC analysis of hydrogen peroxide. Because the reaction rate was the same with or without EDTA when a high purity commercially available deionized ultrafiltered water (DIUF®, see Reagents) was employed, subsequent kinetic studies in which H_2O_2 was monitored were conducted without EDTA addition.

Initial rates of CSSC formation were monitored in solutions at pH 6.0 at a fixed starting concentration of CSH (25 mM), while H_2O_2 starting concentrations were varied or at a fixed starting concentration of H_2O_2 (10 mM) while CSH starting concentrations were varied (see rate law studies). Replicate experiments were performed in air-equilibrated samples and in samples prepared and stored under a nitrogen atmosphere. No significant differences were observed in any of the reactant solutions, indicating that air oxygen is not involved in the reaction between CSH and H_2O_2.

Rate Law, Stoichiometry, and Reaction Mechanism

Prior to generating complete reactant and product concentration versus time profiles for use in quantitative modeling of the reaction, a preliminary study designed to ascertain the reaction order with respect to CSH and H_2O_2 was conducted. Initial rates of formation of CSSC during the first minute after mixing at 25°C were obtained for solutions containing a fixed starting concentration of CSH (25 mM) and varying H_2O_2 concentration (i.e., 5, 10, 25, and 50 mM) or fixed H_2O_2 concentration (10 mM) and varying CSH concentration (i.e., 2, 5, 10, and 25 mM). Plots of CSSC concentration versus time (data not shown) were linear for every combination, but in some cases, particularly at high reactant concentrations, the extent of the reaction as determined by either CSSC formation or loss of CSH exceeded 20%. Therefore, the slopes of the CSSC concentration versus time plots (d[CSSC]/dt) were normalized by dividing by the average concentration of the fixed reactant to adjust for the fact that mean reactant concentrations were less than 100% even during the first minute of the reaction. The slopes obtained appeared to be proportional to the total concentrations of each reactant in all ionization states, $[CSH]_t$ and $[H_2O_2]_t$, indicating that the following rate law may be applicable:

$$d[\mathrm{CSSC}]/dt = k_{\mathrm{obs}}[\mathrm{CSH}]_t[\mathrm{H_2O_2}]_t \qquad (5)$$

Slopes of log–log plots of the normalized rates of CSSC formation versus the variable reactant concentration were 0.96 (±0.01) versus 0.94 (±0.03) for varying H_2O_2 concentrations under nitrogen versus air, respectively, and 0.92 (±0.01) versus 0.92 (±0.02), for varying CSH concentrations under nitrogen versus air, respectively. None of these slopes were significantly different from 1.0 as determined by the overlap of their 95% confidence intervals with 1.0, indicating that the reaction appears to be first-order in terms of each reactant.

A more comprehensive set of experiments was then performed in which the concentrations of CSH, H_2O_2, and CSSC were monitored versus time and fit to the model represented by eqs 1–4 and depicted in Scheme I. Initially, a set of five experiments at a fixed pH (6.0) and CSH concentration (4 mM) and varying concentrations of H_2O_2 (2, 4, 6, 8, and 9.2 mM) were conducted at 25°C so that pH effects could be neglected. Panels representing three of these experiments are shown in Figure 3.

Evident from all three plots, exactly 2 mol of CSH are consumed per mol of H_2O_2, consistent with Scheme I and the overall stoichiometry for the reaction shown below:

$$2\mathrm{CSH} + \mathrm{H_2O_2} \rightarrow \mathrm{CSSC} + \mathrm{H_2O}$$

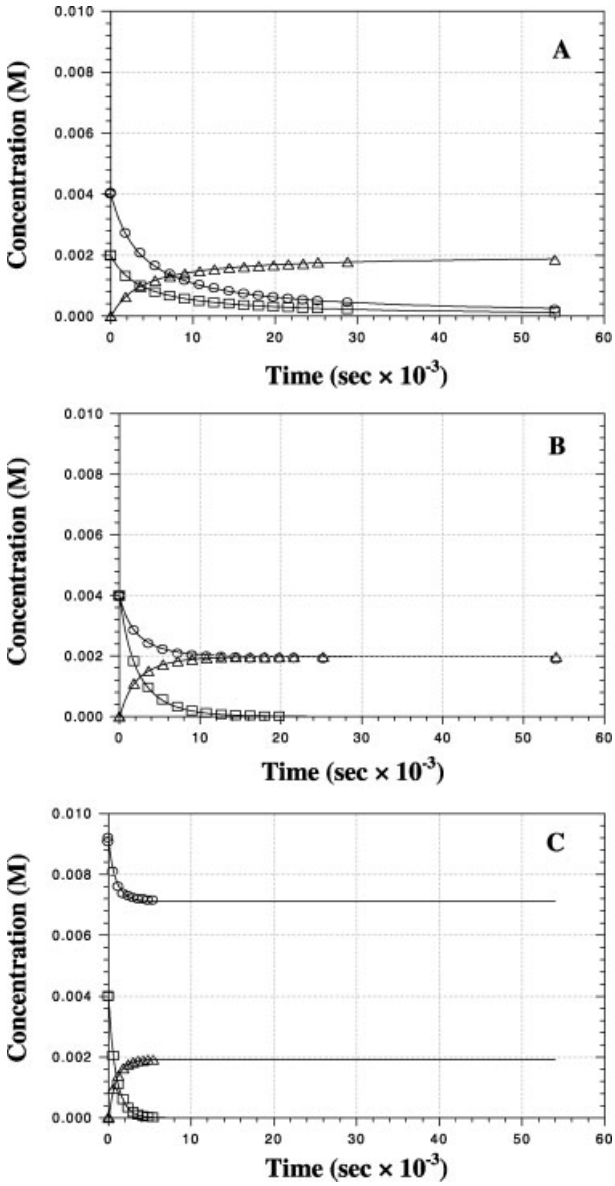

Figure 3. Concentration versus time plots of cysteine (□) cystine (△), and hydrogen peroxide (○) during the reaction of CSH ($[CSH]_0 = 4$ mM) with varying concentrations of H_2O_2 in 50 mM pH 6.0 phosphate buffer at 25°C. (A) $[H_2O_2]_0 = 2$ mM; (B) $[H_2O_2]_0 = 4$ mM; (C). $[H_2O_2]_0 = 9.2$ mM. The curves are nonlinear least-squares best fits using the kinetic model depicted in Scheme I (eqs. 1–4).

The solid curves in Figure 3A–C represent simultaneous nonlinear least-squares fits of the data to the model depicted in Scheme I. Assuming a pKa for the cysteine sulfhydryl ionization of 8.44 (see later discussion), and correcting the pKa for ionic strength, values for the two second-order reaction rate constants at pH 6.0 and 25°C generated through model fitting are $k_1 = 15.2 \pm 0.1\ M^{-1}s^{-1}$, $k_2 = 720 \pm 70\ M^{-1}s^{-1}$. The excellent fit of the data strongly supports the nucleophilic mechanism that Scheme I describes.

The apparent first-order dependence on CSH and H_2O_2 concentrations determined in the initial rate studies can only be consistent with Scheme I if the first step in the reaction, the nucleophilic attack of thiol (or thiolate anion) on H_2O_2 to generate a highly reactive sulfenic acid intermediate is the rate-determining step. The relative values obtained for k_1 and k_2 ($k_1 \ll k_2$) are consistent with the first step being rate-determining. To our knowledge, this is the first attempt to obtain a quantitative estimate for the bimolecular rate constant for thiolate anion attack on cysteine sulfenic acid to generate cystine.

Among those studies in the literature that have concluded that hydrogen peroxide reacts with thiols to produce exclusively the corresponding disulfides there is disagreement as to the reaction stoichiometry and mechanism. Although Darkwa et al.[43] suggested that the oxidation of cysteine by H_2O_2 is predominantly free radical-mediated, most groups have generated results consistent with a two-step nucleophilic substitution mechanism as described in Scheme I.[10,14,15,44] As demonstrated in Figure 3A–C, the overall molar stoichiometry (H_2O_2:RSH) of the nucleophilic mechanism is 1:2. However, Abedinzadeh et al. have argued that this stoichiometry depends on the reactant ratios, such that, at initial reactant concentration ratios $([RSH_0]/[H_2O_2]) > 2.5$ the expected 1:2 stoichiometry is observed while at ratios <2.5 (i.e., excess peroxide) the stoichiometry is 1:1.[41,42] The study described in Figure 3C contained excess peroxide yet the overall stoichiometry remained 1:2.

Abedinzadeh et al.[41,42,53] also reported that the concentration of H_2O_2 undergoes abrupt decreases in the initial stage of reactions between glutathione or N-acetylcysteine, which they attributed to the formation of complexes between RSH and H_2O_2. It is evident in Figure 3A–C that there is no abrupt decrease in hydrogen peroxide concentration in the early stage of this reaction. Moreover, the excellent fit of the data to the model represented in Scheme I, which does not consider complex formation, suggests that a more complicated mechanism is unnecessary. However, apart from the fact that different thiols were the subject of their investigations, Abedinzadeh et al. monitored their reactions using absorbance measurements, whereas these studies employed HPLC.

Further studies are necessary to rationalize these apparently disparate results.

Buffer, Ionic Strength, pH, and Temperature Effects

Parallel experiments were conducted in 50 mM phosphate buffers at different pH values (pH 5, 7, 10, and 13) with or without control of ionic strength. In the absence of ionic strength adjustment, 50 mM phosphate buffers have an ionic strength ranging from 0.05 at pH 4 to 0.43 and pH 13. In the ionic strength-controlled buffer solutions, ionic strength was adjusted to 0.5 M with addition of NaCl. The experimental results in both groups of reactions were similar after correcting for ionic strength effects on pKa values (i.e., no statistically significant difference was observed). The absence of an ionic strength effect on the reaction between CSH and H_2O_2 is consistent with a previous study of the reaction of 2-mercaptoethanol with H_2O_2 as a function of ionic strength over the range of 0.05 M <I <0.4 M reported by Leung et al.[15]

The kinetics of reaction in solutions containing 4 mM CSH and 4 mM H_2O_2 were monitored as a function of buffer concentration in phosphate buffers (pH 7) varying in concentration (10, 30, and 50 mM) and at a constant ionic strength of 0.5 M [adjusted with sodium chloride (NaCl)]. Fitted values of k_1 were 14.0, 17.4, and 20.5 $M^{-1}s^{-1}$ in 10, 30, and 50 mM buffer, respectively. Although the 95% confidence intervals at 10 and 50 mM did not overlap, indicating that the differences were significant, the dominant contribution to k_1 is the nonbuffer-catalyzed reaction.

The influence of pH on the reaction between 4 mM CSH and 4 mM H_2O_2 was monitored at 25°C in buffers ranging in pH from 4–13. Concentration versus time curves such as those shown in Figure 3 were generated at each pH and fit simultaneously to obtain estimates for the thermodynamic pKa values of cysteine and hydrogen peroxide, and values for k_1 and k_2 reflecting the entire pH range. The pKa value found for cysteine, 8.44 ± 0.02, is in reasonable agreement with literature estimates of 8.33[54] and 8.53,[55] while the pKa obtained for H_2O_2, 11.51 ± 0.02, also agrees favorably reported values of 11.45[15] and 11.6.[56] The values found for k_1 ($=14.7 \pm 0.35\ M^{-1}s^{-1}$) and k_2 ($=570 \pm 170\ M^{-1}s^{-1}$) are not significantly different from those obtained at pH 6.0 in which five groups of kinetics experiments varying in CSH and H_2O_2 concentration were analyzed. Shown in Figure 4 is the pH rate profile generated from the pH 4–13 data, where $k_{obs} = k_1 {}^{*}f_{CS^-} {}^{*}f_{HOOH}$ and f_{CS^-} and f_{HOOH} are the fractions of thiolate anion and the neutral species of hydrogen peroxide, determined from their pKa values. The solid line (which was not fitted to the points) in Figure 4 represents the k_1 ($=14.9\ M^{-1}s^{-1}$) obtained from averaging the fits of the pH 4–13 and pH 6 concentration versus time data and the pKa values found from those previous fits (i.e., 8.44 for cysteine and 11.51 for H_2O_2).

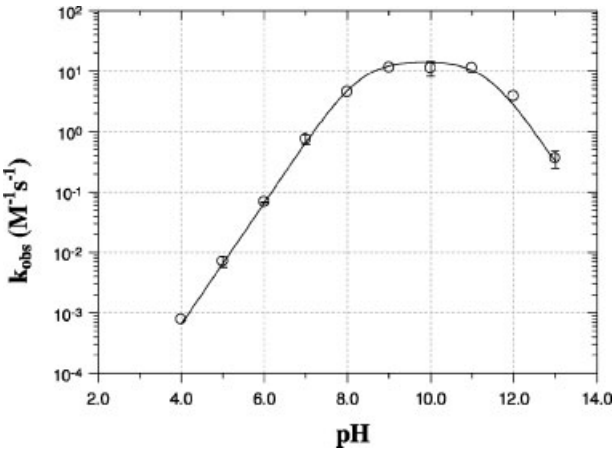

Figure 4. pH dependence of the rate constant for the nucleophilic reaction between cysteine and hydrogen peroxide, k_1, at 25°C.

Our estimate of k_1 ($=14.9\ M^{-1}s^{-1}$) at 25°C appears to be in reasonable accord with literature estimates at other temperatures. Barton et al.[14] obtained a value of 12.4 $M^{-1}s^{-1}$ at room temperature, while Winterbourn and Metodiewa[10] estimated k_1 to be 26 $M^{-1}s^{-1}$ at 37°C. Radi et al.[57] estimated a k_1 of 17.1 $M^{-1}s^{-1}$ at 37°C.

Values of k_1 generated in this study through model fitting at different temperatures from 0–50°C are well described by the Arrhenius equation (Fig. 5) with an activation energy (E_a) of 70.96 kJ/mol (16.96 kcal/mol). Alternatively, use of the Eyring equation yielded an enthalpy of activation, $\Delta H^{\ddagger}$, of 16.4 ± 0.3 kcal/mol and entropy of activation, $\Delta S^{\ddagger}$, of 1.7 ± 1.1 cal $K^{-1}mol^{-1}$. These activation parameters result in an estimated k_1 of 42.6 $M^{-1}s^{-1}$ at 37°C.

The pH profile in Figure 4 covering a range of pH from 4–13 and the kinetic model used to fit these data are consistent with the results of Leung et al.,[15] who examined the reaction of 2-mercaptoethanol with H_2O_2 over the pH range 9–13. These results do not support the conclusions of Barton et al.,[14] who concluded that the rate

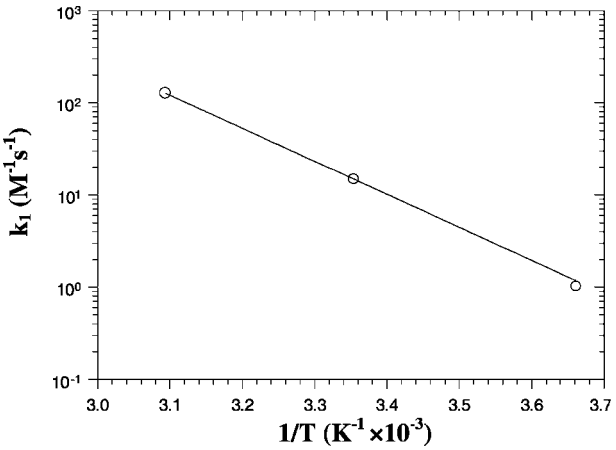

Figure 5. Temperature dependence of the rate constant representing the nucleophilic reaction between cysteine and hydrogen peroxide, k_1.

constant for thiolate anion attack is influenced by the state of ionization of the cysteine amine.

The pH profile shown in Figure 4 is remarkably similar to that reported by Griffths et al. for the oxidation of Cys-232 in recombinant human α1-antitrypsin after correction for the lower pKa of this thiol residue (pKa = 6.86).[5] They obtained a rate constant for the second-order reaction of Cys-232 with H_2O_2 of 7.0 $M^{-1}s^{-1}$ by monitoring the disappearance of the free thiol, because, in this protein, the initial sulfenic acid product of this reaction step is relatively stable. The similarity of our rate constant with that for a cysteine residue in a protein after correcting for pKa differences and the comparison by Winterbourn and Metodiewa[10] of the rate constants for reaction of several low molecular weight thiols with hydrogen peroxide suggest that the thiol pKa is a principal factor determining the relative rates of peroxide-mediated oxidation of thiol residues in peptides and proteins.

Competition Between CSH and H_2O_2 for the Reactive Sulfenic Acid Intermediate (CSOH)

Among previous investigations of the reaction between various low molecular weight thiols (e.g., cysteine, N-acetylcysteine, glutathione, and others) and hydrogen peroxide (H_2O_2) or other peroxides (e.g., benzoyl peroxide, lipid hydroperoxides, etc.) there does not appear to be a consensus as to the reaction products formed under various conditions. Little and O'Brien[39] reported high levels of cysteic acid (RSO_3H) and sulfinic acid (RSO_2H) when cysteine was oxidized with hydrogen peroxide and lipid hydroperoxide, while Finley et al.[40] found that in equimolar aqueous solutions of glutathione and H_2O_2 at varying pH most of the cysteine was oxidized to cystine monoxide or dioxide, along with significant quantities of disulfide (RSSR) formation. In contrast, several groups have reported that the exclusive product formed between hydrogen peroxide and cysteine, glutathione, N-acetylcysteine, and other thiols is the disulfide.[10,14,15,41,42]

The agreement of the previous experimental data generated at pH 6.0 and 4 mM CSH with H_2O_2 concentrations ranging from 2 to 9.2 mM as well as the agreement of the pH profile in Figure 4 with the mathematical model derived from the two-step nucleophilic reaction mechanism depicted in Scheme I strongly support this mechanism. However, CSOH is itself quite reactive,[44] and can participate in several additional reactions as shown in Scheme II. These include the condensation reaction between two CSOH molecules to form a thiolsulfinate[58] and nucleophilic attack of H_2O_2 by CSOH to form the sulfinic acid (CSO_2H), which can then undergo reaction with another molecule of H_2O_2 to form a sulfonic acid (cysteic acid, CSO_3H).[5]

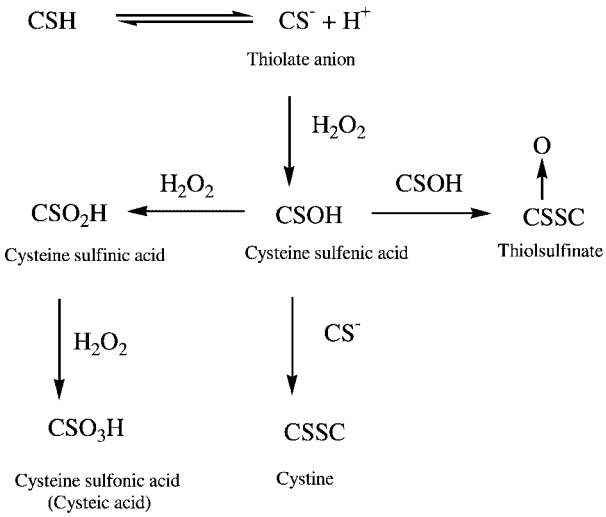

Scheme II.

To explore the range of concentration ratios over which Scheme I accounts for the reaction kinetics, additional experiments were conducted in which the ratios were varied over a much wider range. One experiment employed a 100-fold excess of CSH using 500 μM H_2O_2 to react with 50 mM CSH. Presented in Figure 6 is a semilogarithmic plot of the $[H_2O_2]$ versus time from which a value of $k_1 = 15.04 \pm 1.55$ $M^{-1}s^{-1}$ was obtained. Scheme I thus seems to be applicable over a wide range of concentration ratios when CSH is in excess.

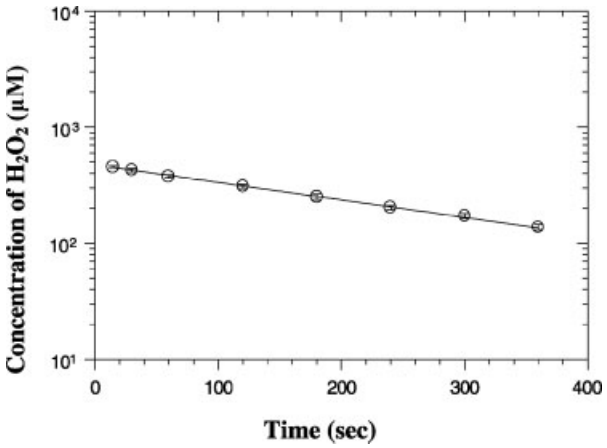

Figure 6. Semilogarithmic plot of the disappearance of H_2O_2 versus time in the reaction between 50 mM CSH and 500 μM H_2O_2 in 50 mM pH 6.0 aqueous phosphate buffer at 25°C.

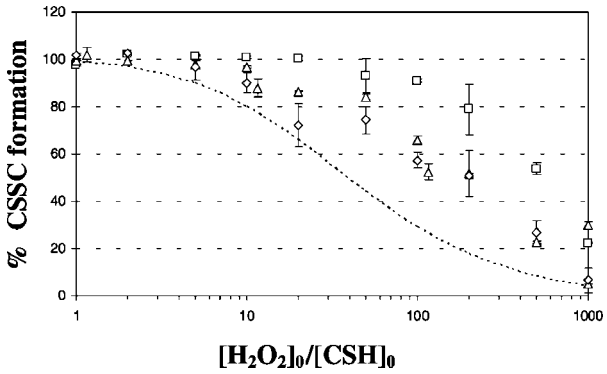

Figure 7. The dependence of percentage of CSSC formed on the $[H_2O_2]_0/[CSH]_0$ starting concentration ratio in 50 mM phosphate buffer at 25°C. Key: (□), pH 5; (◇), pH 6; (△), pH 7. The dashed line is simulated from the model depicted in Scheme I.

Scheme II implies that when H_2O_2 is present in large excess, competition for the reactive intermediate CSOH will lead to the formation of multiple reaction products and a reduction in the fraction of disulfide product. Shown in Figure 7 is the % CSSC formed at the completion of the reaction in phosphate buffers at pH 5.0, 6.0, and 7.0 versus the starting concentration ratio $[H_2O_2]_0/[CSH]_0$ which was varied from 1:1 to 1000:1. These results indicate that the higher the starting concentration ratio, the lower the percentage of CSSC formed in comparison to the stoichiometric amount. When the starting concentration ratio between H_2O_2 and CSH reaches 1000:1, the overall reaction is diverted to other products such as cysteine sulfinic acid and cysteic acid, consistent with Scheme II.

The dashed line in Figure 7 represents the predicted % CSSC formed at the completion of the reaction according to the mathematical model described in eqs. 1–4 representing Scheme I. This model, which ignores the potential competition between CSH and other species for the reactive intermediate nevertheless predicts a decline in the percentage of disulfide forming at the end of the reaction because of the depletion in concentration of CSH necessary to convert CSOH to CSSC at high concentrations of H_2O_2, resulting in a predicted buildup of the reactive intermediate CSOH. Interestingly, this model underestimates the % CSSC formed at high $[H_2O_2]_0/[CSH]_0$ ratios, indicating that additional pathways may exist for the generation of CSSC besides that depicted in Schemes I and II. A possible additional route for generation of CSSC may involve hydrolysis of the thiolsulfinate to produce cysteine, which is then available to participate in the reaction cycle in Scheme I:

$$CSOSC + H_2O \rightarrow CSO_2H + CSH$$

Sohn and Rudolph[59] found that thiosulfinate hydrolysis was necessary to include to account for the kinetics of oxidation/reduction reactions in the Cdc25 phosphatases, which belong to the family of protein tyrosine phosphatases that contain an active-site cysteine residue.

The predominance of the disulfide reaction product (except at extremely high ratios of $[H_2O_2]_0/[CSH]_0$) in the reaction of cysteine and hydrogen peroxide in aqueous buffers is consistent with several reports on the reaction of thiol containing proteins with hydrogen peroxide, where the final product is a disulfide because of the proximity of adjacent thiol-containing residues.[59–61] In other cases, however, sulfenic, sulfinic, and sulfonic acids or other reaction products dominate.

Functional protein sulfenic acids may play important roles in various cellular processes, including signal transduction, oxygen metabolism and the oxygen stress response, and transcriptional regulation.[8] The cellular redox state appears to be involved in the regulation of catalytic activity of thiol-dependent enzymes through reversible sulfenic acid formation at catalytic cysteine residues. The only free thiol residue in human serum albumin, Cys34, reacts with hydrogen peroxide to form a remarkably stable sulfenic acid intermediate, with only ~15% decaying after

2 h at 37°C. Griffiths et al.[5] noted that the sulfenic acid intermediate formed in the oxidation of the Cys-232 residue in recombinant human α1-antitrypsin is not sufficiently stable to preclude further oxidation to sulfinic and cysteic acids. On the other hand, Montfort et al. have suggested that irreversible formation of sulfinic and sulfonic acids is prevented in protein tyrosine phosphatase enzymes by formation of a sulphenyl amide intermediate.[62]

SUMMARY

Kinetic studies in aqueous buffers over a wide pH range (4–13) and $[H_2O_2]_0/[CSH]_0$ ratios varying from 0.01–2.3 demonstrate that the reaction of cysteine with hydrogen peroxide in the absence of metal ions is quantitatively consistent with a two-step nucleophilic reaction mechanism in which the nucleophilic attack of thiolate anion on the unionized H_2O_2 species is rate-determining. Values of the two second-order reaction rate constants generated through model fitting of five groups of data at 25°C and pH 6.0 are $k_1 = 15.2 \pm 0.1$ $M^{-1}s^{-1}$ and $k_2 = 720 \pm 70$ $M^{-1}s^{-1}$ agreed reasonably well with estimates of 14.7 ± 0.35 $M^{-1}s^{-1}$ and 570 ± 170 $M^{-1}s^{-1}$ obtained from fitting the entire pH rate profile between pH 4–13.

At starting concentration ratios, $[H_2O_2]_0/[CSH]_0 > 10$, the % disulfide formation declines due to CSH depletion or the increased importance of alternative pathways for consumption of CSOH that compete with the formation of CSSC from CSH + CSOH. The generation of the reactive sulfenic acid intermediate and its fate are of increasing biological interest because these reactions may regulate a wide array of cellular processes that respond to the intracellular redox status. The increased stability of the sulfenic acid intermediate in proteins may be related to such factors as hydrogen bonding to neighboring substituents in the protein or limited access of neighboring protein thiol residues or low molecular weight thiols present in cells to the site of oxidation due to conformational or steric constraints. Related factors (e.g., limited proximity and mobility) may also determine the fate of reactions of thiol containing drugs, including peptides and proteins, in amorphous pharmaceutical formulations such as lyophilized formulations. Current studies in these laboratories are aimed at elucidating the influence of such factors on thiol oxidation in solid-state formulations. A thorough understanding of the mechanism in aqueous solution will provide valuable background information for this undertaking.

ACKNOWLEDGMENTS

This work was supported by a grant from Pfizer Inc. We thank Drs. Paul Bummer and Tian-xiang Xiang for their helpful advice and discussions.

REFERENCES

1. Ahern TJ, Manning MC. 1992. Stability of protein pharmaceuticals. Part A: Chemical and physical pathways of protein degradation. New York: Plenum Press.
2. Wang YJ, Pearlman R. 1993. Stability and characterization of protein and peptide drugs: Case histories. New York: Plenum Press.
3. Volkin DB, Mach H, Middaugh RC. 1997. Degradative covalent reactions important to protein stability. Mol Biotechnol 8:105–122.
4. Carballal S, Radi R, Kirk MC, Barnes S, Freeman BA, Alvarez B. 2003. Sulfenic acid formation in human serum albumin by hydrogen peroxide and peroxynitrite. Biochemistry 42:9906–9914.
5. Griffiths SW, King J, Cooney CL. 2002. The reactivity and oxidation pathway of cysteine 232 in recombinant human α1-antitrypsin. J Biol Chem 277:25486–25492.
6. Denu JM, Tanner KG. 1998. Specific and reversible inactivation of protein tyrosine phosphatases by hydrogen peroxide: Evidence for a sulfenic acid intermediate and implications for redox regulation. Biochemistry 37:5633–5642.
7. Caselli A, Marzocchini R, Camici G, Manao G, Moneti G, Pieraccini G, Ramponi G. 1998. The inactivation mechanism of low molecular weight phosphotyrosine-protein phosphatase by H_2O_2. J Biol Chem 273:32554–32560.
8. Claiborne A, Yeh JI, Mallett TC, Luba J, Crane EJ III, Charrier V, Parsonage D. 1999. Protein-sulfenic acids: Diverse roles for an unlikely player in enzyme catalysis and redox regulation. Biochemistry 38:15407–15416.
9. Winterbourn CC, Metodiewa D. 1994. The reaction of superoxide with reduced glutathione. Arch Biochem Biophys 314:284–290.
10. Winterbourn CC, Metodewa D. 1999. Reactivity of biologically important thiol compounds with superoxide and hydrogen peroxide. Free Radic Biol Med 27:322–328.
11. Lee T-Y, Notari RE. 1987. Kinetics and mechanism of captopril oxidation in aqueous solution under controlled oxygen partial pressure. Pharm Res 4:98–103.

12. Terasawa H, Tsang K-Y, Gulley J, Arlen P, Schlom J. 2002. Identification and characterization of a human agonist cytotoxic T-lymphocyte epitope of human prostate-specific antigen. Clin Cancer Res 8:41–53.
13. Aruoma OI, Halliwell B, Hoey BM, Butler J. 1989. The antioxidant action of N-acetylcysteine: Its reaction with hydrogen peroxide, hydroxyl radical, superoxide, and hypochlorous acid. Free Radic Biol Med 6:593–597.
14. Barton JP, Packer JE, Sims RJ. 1973. Kinetics of the reaction of hydrogen peroxide with cysteine and cysteamine. J Chem Soc Perkin Trans II:1547–1549.
15. Leung P-SK, Hoffmann MR. 1985. Kinetics and mechanism of the oxidation of 2-mercaptoethanol by hydrogen peroxide in aqueous solution. J Phys Chem 89:5267–5271.
16. Johnson DM, Gu L. 1988. Autoxidation and antioxidants. In: Swarbrick J, Boylan JC, editors. Encyclopedia of pharmaceutical technology. New York: Marcel Dekker, Inc., pp 415–449.
17. Caraballo I, Rabasco AM, Fernandez-Arevalo M. 1993. Study of thimerosal degradation mechanism. Int J Pharm 89:213–221.
18. Akers MJ. 1982. Antioxidants in pharmaceutical products. J Parenteral Sci Tech 36:222–228.
19. Knepp VM, Whatley JL, Muchnik A, Calderwood TS. 1996. Identification of antioxidants for prevention of peroxide-mediated oxidation of recombinant human ciliary neurotrophic factor and recombinant human nerve growth factor. PDA J Pharmaceut Sci Technol 50:163–171.
20. Strickley RG, Anderson BD. 1993. Solubilization and stabilization of an anti-HIV thiocarbamate, NSC 629243, for parenteral delivery using extemporaneous emulsions. Pharm Res 10:1076–1082.
21. Cullis CF, Hopton JD, Swan CJ, Trimm DL. 1968. Oxidation of thiols in gas–liquid systems. II. Reaction in the presence of added metal catalysts. J Appl Chem 18:335–339.
22. Ehrenberg L, Harms-Ringdahl M, Fedorcsak I, Granath F. 1989. Kinetics of the copper- and iron-catalysed oxidation of cysteine by dioxygen. Acta Chem Scand 43:177–187.
23. Gupta S, Anderson BD. 1998. Oxidation mechanism of thiol-containing PSA peptide in aqueous solutions in the presence of oxygen and cupric ions. AAPS PharmSci 1:S-262.
24. Gu L, Fausnaugh J. 1993. Stability and characterization of human interleukin-1b. In: Wang YJ, Pearlman R, editors. Stability and characterization of protein and peptide drugs. New York: Plenum Press, pp 221–248.
25. Gupta S, Morgan ME, Anderson BD. 1997. Evaluation of two experimental design methods for optimizing formulations of thiol-containing peptides susceptible to oxidation. Pharm Res 14:S158.
26. Bhandarkar SV, Anderson BD. 1999. Oxidation of PSA-OP (NSC 694156), a novel, thiol-containing prostate specific antigen. AAPS PharmSci 1(4).
27. Ha E, Wang W, Yang YJ. 2002. Peroxide formation in polysorbate 80 and protein stability. J Pharm Sci 91:2252–2264.
28. Hartauer KJ, Arbuthnot GN, Baertschi SW, Johnson RA, Luke WD, Pearson NG, Rickard EC, Tingle CA, Tsang P-KS, Wiens RE. 2000. Influence of peroxide impurities in povidone and crospovidone on the stability of raloxifene hydrochloride in tablets: Identification and control of an oxidative degradation product. Pharm Dev Technol 5:303–310.
29. Ding S. 1993. Quantitation of hydroperoxides in the aqueous solutions of non-ionic surfactants using polysorbate 80 as the model surfactant. J Pharm Biomed Anal 2:95–101.
30. McGinity JW, Hill JA, La Via AL. 1975. Influence of peroxide impurities in polyethylene glycols on drug stability. J Pharm Sci 64:356–357.
31. McGinity JW, Patel TR, Tarun R, Naqvi AH, Hill JA. 1976. Implications of peroxide formation in lotion and ointment dosage forms containing polyethylene glycols. Drug Dev Commun 2:505–519.
32. Rieger MM. 1975. Peroxides in polyethylene glycols and polyethyleneglycol derivatives. Cosmet Perfum 90:13–16.
33. Magill A, Becker AR. 1984. Spectrophotometric method for quantitation of peroxides in sorbitan monooleate and monostearate. J Pharm Sci 73: 1663–1664.
34. Huang T, Garceau ME, Gao P. 2003. Liquid chromatographic determination of residual hydrogen peroxide in pharmaceutical excipients using platinum and wired enzyme electrodes. J Pharm Biomed Anal 31:1203–1210.
35. Huang X, Atwood CS, Hartshorn MA, Multhaup G, Goldstein LE, Scarpa RC, Cuajungco MP, Gray DN, Lim J, Moir RD, Tanzi RE, Bush AI. 1999. The Ab peptide of Alzheimer's disease directly produces hydrogen peroxide through metal ion reduction. Biochemistry 38:7609–7616.
36. Hanaki A, Kamide H. 1983. The copper-catalyzed autoxidation of cysteine. The amount of hydrogen peroxide produced under various conditions and the stoichiometry of the reaction. Bull Chem Soc Jpn 56:2065–2068.
37. Kachur AV, Koch CJ, Biaglow JE. 1998. Mechanism of copper-catalyzed oxidation of glutathione. Free Radic Res 28:259–269.
38. Correale P, Walmsley K, Nieroda C, Zaremba S, Zhu M, Schlom J, Tsang KY. 1997. In vitro generation of human cytotoxic T lymphocytes specific for peptides derived from prostate-specific antigen. J Natl Cancer Inst 89: 293–300.

39. Little C, O'Brien PJ. 1967. Products of oxidation of a protein thiol group after reaction with various oxidizing agents. Arch Biochem Biophys 122:406.
40. Finley JW, Wheeler EL, Witt SC. 1981. Oxidation of glutathione by hydrogen peroxide and other oxidizing agents. J Agric Food Chem 29:404–407.
41. Abedinzadeh Z, Gardes-Albert M, Ferradini C. 1989. Kinetic study of the oxidation mechanism of glutathione by hydrogen peroxide in neutral aqueous medium. Can J Chem 67:1247–1255.
42. Abedinzadeh Z, Arroub J, Gardes-Albert M. 1994. On N-acetylcysteine. Part II. Oxidation of N-acetylcysteine by hydrogen peroxide: Kinetic study of the overall process. Can J Chem 72:2102–2107.
43. Darkwa J, Mundoma C, Simoyi RH. 1998. Antioxidant chemistry. Reactivity and oxidation of DL-cysteine by some common oxidants. J Chem Soc Faraday Trans 94:1971–1978.
44. Barrett GC. 1990. Structural Chemistry. In: Patai S, editor. The chemistry of sulfenic acids and their derivatives. New York: John Wiley and Sons, pp 1–22.
45. Neville RG. 1957. The oxidation of cysteine by iron and hydrogen peroxide. J Am Chem Soc 79:2456–2457.
46. Vignaud C, Rakotozafy L, Falguieres A, Potus J, Nicolas J. 2004. Separation and identification by gel filtration and high-performance liquid chromatography with UV or electrochemical detection of the disulphides produced from cysteine and glutathione oxidation. J Chromatogr A 1031:125–133.
47. Nahum A, Wood LDH, Sznajder JI. 1989. Measurement of hydrogen peroxide in plasma and blood. Free Radic Biol Med 6:479–484.
48. Schöneich C, Hageman MJ, Borchardt RT. 1997. Stability of peptides and proteins. In: Park K, editor. Controlled drug delivery challenges and strategies. Washington, DC: American Chemical Society, pp 205–228.
49. Hanaki A, Kamide H. 1973. Participation of Cu (II) ion in the oxidation of cysteine with hydrogen peroxide. Chem Pharm Bull 21:1421–1425.
50. Pecci L, Montefoschi G, Musci G, Cavallini D. 1997. Novel findings on the copper catalysed oxidation of cysteine. Amino Acids 13:355–367.
51. Smith RC, Reed VD, Hill WE. 1994. Oxidation of thiols by copper(II). Phosphorus Sulfur Silicon 90:147–154.
52. Zwart J, Van Wolput JHMC, Koningsberger DC. 1981. The mechanism of the copper ion catalyzed autoxidation of cysteine in alkaline medium. J Mol Catal 12:85–101.
53. Arroub J, Berges J, Abedinzadeh Z, Langlet J, Gardes-Albert M. 1994. On N-acetylcysteine. Part I. Experimental and theoretical approaches of the N-acetylcysteine/H_2O_2 complexation. Can J Chem 72:2094–2101.
54. 1989. The Merck Index. Rahway, NJ: Merck & Co., Inc., p 436.
55. Benesch RE, Benesch R. 1955. The acid strength of the −SH group in cysteine and related compounds. J Am Chem Soc 77:5877.
56. CRC Handbook of Chemistry and Physics. 2001. Cleveland, OH: CRC Press.
57. Radi R, Beckman JS, Bush KM, Freeman BA. 1991. Peroxynitrite oxidation of sulfhydryls—The cytotoxic potential of superoxide and nitric oxide. J Biol Chem 266:4244–4250.
58. Kice JL. 1980. Mechanisms and reactivity in reactions of organic oxyacids of sulfur and their anhydrides. Adv Phys Org Chem 17:65–181.
59. Sohn J, Rudolph J. 2003. Catalytic and chemical competence of regulation of Cdc25 phosphatase by oxidation/reduction. Biochemistry 42: 10060–10070.
60. Shen H, Tsuchida S, Tamai K, Sato K. 1993. Identification of cysteine residues involved in disulfide formation in the inactivation of glutathione transferase P-form by hydrogen peroxide. Arch Biochem Biophys 300:137–141.
61. Ellis HR, Poole LB. 1997. Roles for the two cysteine residues of AhpC in catalysis of peroxide reduction by alkyl hydroperoxide reductase from *Salmonella typhimurium*. Biochemistry 36:13349–13356.
62. Montfort RLM, Congreve M, Tisi D, Carr R, Jhoti H. 2003. Oxidation state of the active-site cysteine in protein tyrosine phosphatase 1B. Nature 423: 773–777.